Minimization of thin film contact resistance

Peng Zhang, Y. Y. Lau,[a] and R. M. Gilgenbach
Department of Nuclear Engineering and Radiological Sciences, University of Michigan, Ann Arbor, Michigan 48109-2104, USA

(Received 21 September 2010; accepted 27 October 2010; published online 19 November 2010)

The geometry that minimizes the electrical constriction resistance of thin film contact is identified for both Cartesian and cylindrical geometries. Assuming uniform resistivity on an idealized model, simple scaling laws for the thin film contact resistance are constructed, for arbitrary ratio of constriction size to film thickness. Optimal conditions to minimize the thin film contact resistance are identified. The analytic calculations are confirmed with numerical code results. © *2010 American Institute of Physics*. [doi:10.1063/1.3517497]

Thin film contact is a very important issue in various areas, such as integrated circuits,[1,2] thin film devices,[3,4] carbon nanotube and carbon nanofiber based cathodes[5,6] and interconnects,[5,7] field emitters,[6,8] and thin film-to-bulk contacts,[9] etc. The two-dimensional (2D) thin film resistance has been investigated for various patterns in Cartesian geometry.[3] The spreading resistance of three-dimensional (3D) thin film disks is also analyzed.[9,10] However, there is a lack of analytical scaling that readily gives an explicit evaluation of thin film contact resistance. Few theoretical studies focus on optimization of the thin film pattern that minimizes this contact or constriction resistance. This paper addresses these issues.

Holm's classical *a*-spot theory of electrical contact resistance[11] has been extended to include the effects of finite bulk radius,[12] of finite thickness of contact "bridge,"[13,14] and of dissimilar materials and contaminants.[15] These prior works are inapplicable to the thin film geometry that is studied in this paper (Fig. 1). This is particularly the case when the ratio of the constriction radius (a) to the film thickness (h) is on the order of unity, where the current is mostly confined to the immediate vicinity of the constriction and flows parallel to the thin film boundary.

Both Cartesian and cylindrical geometries of the thin film are shown in Fig. 1. The current flows inside the base thin film, converging toward the center of the joint region, and feeds into the top channel. This configuration is representative to various applications. The Cartesian case may represent a thin film sheet resistor,[3] where the third dimension, which is perpendicular to the plane of the paper, is small. It may also represent a heatsink geometry, where this third dimension is large. The cylindrical case may represent a carbon nanotube[5–8] or a field emitter[6] setting on a substrate or it may represent a Z-pinch wire connected to a plate electrode.[16] With the assumption of uniform resistivity, we will study the dependence of the constriction resistance on the geometries shown in Fig. 1. We shall determine the conditions under which the thin film constriction or contact resistance is minimized.

Consider first the 2D Cartesian "T"-shape thin film pattern (Fig. 1). The base region has width h, and the top region has half width a. The pattern is symmetrical about the vertical center axis. Current flows from the two terminals E and F to the top terminal GH. The resistivity ρ is assumed constant for the whole pattern. We also assume that $L_2 \gg h$, $L_2 \gg a$, and $L_1 \gg a$, so that the current flows are uniform at all the ends E, F, G, and H, far from the joint region. The total resistance R from EF to GH is found to be

$$R = \frac{\rho L_2}{2h \times W} + \frac{\rho}{4\pi W}\bar{R}_c\left(\frac{a}{h}\right) + \frac{\rho L_1}{2a \times W}, \tag{1}$$

where W denotes the channel width in the third, ignorable dimension that is perpendicular to the paper, and the rest of the symbols have been defined in Fig. 1. In Eq. (1), the first term represents the bulk resistance of the thin film base, from A to F, and from D to E. The third term represents the bulk resistance of the top region from B to G. The second term represents the remaining constriction resistance R_c for the region ABCD.

If we express the constriction (contact) resistance as $R_c = (\rho/4\pi W)\bar{R}_c$ for the Cartesian case, we find that $\bar{R}_c$ depends only on the aspect ratio a/h, as explicitly shown in Eq. (1). The *exact* expression for $\bar{R}_c$ can be simply derived from conformal mapping[3,13,17]

$$\bar{R}_c\left(\frac{a}{h}\right) = 4\ln\left[\frac{1}{4}\left(\frac{a}{h}+\frac{h}{a}\right)\right] + 4\left(\frac{h}{a}\right)\tan^{-1}\left(\frac{a}{h}\right) + 4\left(\frac{a}{h}\right)\tan^{-1}\left(\frac{h}{a}\right), \tag{2}$$

which is plotted in Fig. 2. For $a/h > 1$, $\bar{R}_c$ increases as a/h increases. For $a/h < 1$, $\bar{R}_c$ increases as a/h decreases. This behavior is easily understood since the current flow paths

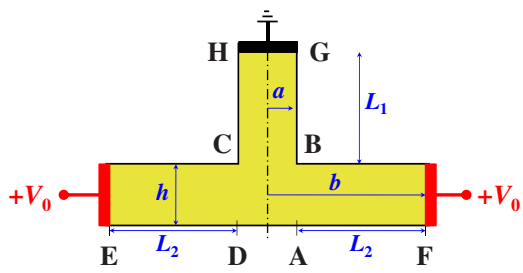

FIG. 1. (Color online) Thin film structures in either Cartesian or cylindrical geometries. Terminals E and F are held at a constant voltage (V_0) relative to terminal GH, which is grounded. The vertical dash-dot line is the axis of rotation for the cylindrical geometry.

[a]Electronic mail: yylau@umich.edu.

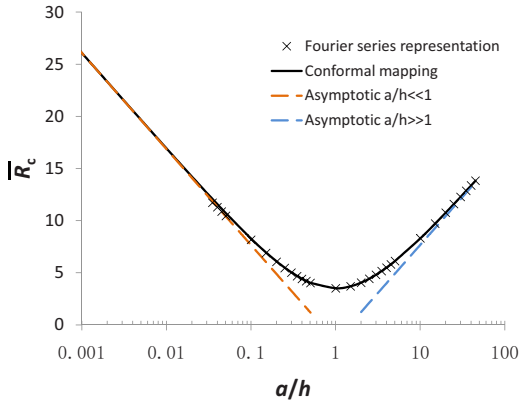

FIG. 2. (Color online) $\bar{R}_c$ as a function of a/h, for the Cartesian structure in Fig. 1. The solid line represents the conformal mapping results [Eq. (2)], the dashed lines represent the asymptotes [Eq. (3)], and the symbols represents the Fourier series representation calculation.

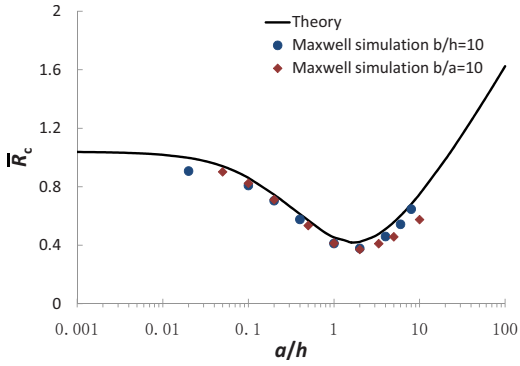

FIG. 3. (Color online) $\bar{R}_c$ as a function of a/h, for the cylindrical structure in Fig. 1. The theoretical result (line) [Eq. (5)] is compared to MAXWELL 3D simulation (symbols). In the simulation, we set $\rho=0.001\ \Omega$m, $L_1=10$ mm, a ranging from 0.01 to 4 mm with fixed $b=10h=5$ mm, and h ranging from 0.1 to 20 mm with fixed $b=10a=10$ mm, and a terminal voltage $V_0=10$ V was applied.

will be lengthened whenever the aspect ratio of a/h deviates from 1. Thus, the constriction (contact) resistance is minimized when $a=h$, at which $\bar{R}_c=2\pi-4\ln 2=3.5106$. Taylor expansion of Eq. (2) yields the asymptotic expressions

$$\bar{R}_c \cong -4\ln(a/h) - 8\ln 2 + 4, \quad a/h \ll 1,$$

$$\bar{R}_c \cong 4\ln(a/h) - 8\ln 2 + 4, \quad a/h \gg 1 \tag{3}$$

which are also shown in Fig. 2.

Since the cylindrical geometry shown in Fig. 1 cannot be solved by conformal mapping, we shall use a Fourier representation for the solutions in the cylindrical tube at the top, and in the circular disk at the bottom, and then match the solutions at the interface BC. This procedure extends the one given in Appendix A of Ref. 15, and will be published elsewhere. As a validation, we have applied this Fourier representation technique to the Cartesian geometry and compared with the results obtained from conformal mapping. This comparison is also shown in Fig. 2. Excellent agreement is noted. This validation added confidence on the Fourier representation method as applied to the cylindrical geometry, reported below.

In the cylindrical configuration (Fig. 1), a long cylindrical rod of radius a is standing on the center of large thin-film circular disk of thickness h and radius $b=a+L_2$. Current flows inside the thin-film disk, from circular rim, E and F, to terminal GH. Once more, we assume $L_1 \gg a$, $L_2 \gg a$, and $L_2 \gg h$, so that the current flow is uniform at F and G, far from the constriction region ABCD. For constant resistivity ρ the total resistance R from EF to GH is found to be

$$R = \frac{\rho}{2\pi h}\ln\left(\frac{b}{a}\right) + \frac{\rho}{4a}\bar{R}_c\left(\frac{a}{h}\right) + \frac{\rho L_1}{\pi a^2}. \tag{4}$$

In Eq. (4), the first term represents the bulk resistance of the thin film, exterior to the constriction region ABCD. It is simply the resistance of a disk of inner radius a, outer radius b, and thickness h.[9] The third term represents the bulk resistance of the top cylinder, BCHG. The second term represents the remaining constriction resistance R_c for the region ABCD. The constriction (contact) resistance is expressed as $R_c=(\rho/4a)\bar{R}_c$ for the cylindrical case. The theoretical result for $\bar{R}_c$, obtained from the Fourier representation method, is shown by the solid curve in Fig. 3. This curve may be fitted with the following formula:

$$\bar{R}_c \cong 1.0404 - 2.2328x + 5.0695x^2 - 7.5890x^3 + 6.5898x^4 - 2.9466x^5 + 0.5226x^6,$$
$$x = a/h, a/h \le 1.6,$$

$$\bar{R}_c \cong 0.4571 - 0.1588y + 0.1742y^2 - 0.0253y^3 + 0.0015y^4, \quad y = \ln(a/h), 1.6 < a/h < 100. \tag{5}$$

Equation (5) is accurate to within 1% in representing the Fourier analysis results for $a/h<100$. We should emphasize that we have not established the asymptotic dependence of $\bar{R}_c$ as $a/h \to \infty$.

It is natural to anticipate that when $L_2 \gg h$, $L_2 \gg a$, and $L_1 \gg a$, $\bar{R}_c$ depends only on the aspect ratio a/h, as shown in Eq. (4) and Fig. 3. These conditions guarantee that the current flows are uniform at F and G, far away from the constriction region. Thus, the normalized contact resistance $\bar{R}_c$, which arises primarily in the immediate vicinity of the constriction edge, is independent of b. Somewhat unexpectedly, our Fourier representation data reveal that the sole dependence of $\bar{R}_c$ on a/h is observed for a much broader range of parameters, as long as either $L_2 \gg a$ or $L_2 \gg h$. This is probably due to the fact that if $L_2 \gg a$, the electrostatic fringe field at the corner B (Fig. 1) is restricted to a distance of at most a few a's, making the flow field at the terminal F insensitive to b. Likewise, if $L_2 \gg h$, the electrostatic fringe field at the corner B is restricted to a distance of at most a few h's, making the flow field at the terminal F also insensitive to b. Thus, for a given ratio of a/h, Eq. (5) may be readily used to evaluate the corresponding constriction (contact) resistance R_c, provided $L_1 \gg a$, and either $L_2 \gg h$ or $L_2 \gg a$.

Figure 3 shows that there is also a minimum value of $\bar{R}_c$ for the cylindrical geometry. This minimum value is 0.42, occurring at $a/h \cong 1.6$. The cylindrical case differs from the Cartesian case in one aspect, namely, as $a/h \to 0$, our numerical calculations show that $\bar{R}_c$ converges to a constant value of about 1.04. The explanation follows. If $a/h \to 0$, both the radius and thickness of the film region are much larger than the radius a of the top cylinder, as if two semi-

infinite long cylinders are joining together with radius ratio of $b/a \to \infty$. In this case, the a-spot theory[11] gives a value of $\bar{R}_c$ of 1.0404, for a uniform resistivity over the whole current channel [c.f. Eq. (2) of Ref. 15].

The calculated $\bar{R}_c$ is also spot-checked against MAXWELL 3D code[18] with several combinations of a, h, and b, as shown in Fig. 3. Good agreement is noted in general. The discrepancies, e.g., in the leftmost and rightmost data point in Fig. 3, are due to the large contrasts in the dimensions (L_1, b, a, h), as well as insufficiently fine meshing of the MAXWELL 3D code, for which the MAXWELL 3D code results are less accurate.

In this paper, analytic scalings for the constriction (or contact) resistance of thin films are presented, for both Cartesian and cylindrical configurations. For the Cartesian case, $\bar{R}_c$ is minimized at $a/h=1$. If a/h deviates from 1, $\bar{R}_c$ increases logarithmically. For the cylindrical case, minimum $\bar{R}_c$ occurs at $a/h=1.6$. In the limit $a/h \to 0$, $\bar{R}_c$ converges to the known limit of 1.0404. Our analysis here may readily be adapted to thermal conduction in thin film structures under steady state. It could also be applicable to the maximization of channel flow at a given pressure.

This work was supported by an AFOSR grant on the Basic Physics of Distributed Plasma Discharges, L-3 Communications Electron Device Division, and Northrop-Grumman Corporation. One of us (P.Z.) gratefully acknowledges a fellowship from the University of Michigan Institute for Plasma Science and Engineering.

[1]G. H. Gelinck, T. C. T. Geuns, and D. M. de Leeuw, Appl. Phys. Lett. **77**, 1487 (2000); W. J. Greig, *Integrated Circuit Packaging, Assembly, and Interconnections* (Springer, New York, 2007).
[2]J. L. Carbonero, G. Morin, and B. Cabon, IEEE Trans. Microwave Theory Tech. **43**, 2786 (1995).
[3]P. M. Hall, Thin Solid Films **1**, 277 (1968); **300**, 256 (1997).
[4]H. Klauk, G. Schmid, W. Radlik, W. Weber, L. Zhou, C. D. Sheraw, J. A. Nichols, and T. N. Jackson, Solid-State Electron. **47**, 297 (2003).
[5]R. H. Baughman, A. A. Zakhidov, and W. A. de Heer, Science **297**, 787 (2002).
[6]D. Shiffler, T. K. Statum, T. W. Hussey, O. Zhou, and P. Mardahl, in *Modern Microwave and Millimeter Wave Power Electronics*, edited by R. J. Barker, J. H. Booske, N. C. Luhmann, and G. S. Nusinovich (IEEE, Piscataway, 2005), Chap. 13, p. 691; V. Vlahos, J. H. Booske, and D. Morgan, Appl. Phys. Lett. **91**, 144102 (2007).
[7]W. Wu, S. Krishnan, T. Yamada, X. Sun, P. Wilhite, R. Wu, K. Li, and C. Y. Yang, Appl. Phys. Lett. **94**, 163113 (2009); Z. Yao, C. L. Kane, and C. Dekker, Phys. Rev. Lett. **84**, 2941 (2000); D. Mann, A. Javey, J. Kong, Q. Wang, and H. Dai, Nano Lett. **3**, 1541 (2003).
[8]R. Miller, Y. Y. Lau, and J. H. Booske, Appl. Phys. Lett. **91**, 074105 (2007).
[9]R. Timsit, Proceedings of the 54th IEEE Holm Conference on Electrical Contacts, 2008, pp. 332–336; M. B. Read, J. H. Lang, A. H. Slocum, and R. Martens, Proceedings of the 55th IEEE Holm Conference on Electrical Contacts, 2009, pp. 303–309; G. Norberg, S. Dejanovic, and H. Hesselbom, IEEE Trans. Compon. Packag. Technol. **29**, 371 (2006).
[10]M. W. Denhoff, J. Phys. D: Appl. Phys. **39**, 1761 (2006).
[11]R. Holm, *Electric Contact*, 4th ed. (Springer, Berlin, 1967).
[12]R. S. Timsit, IEEE Trans. Compon. Packag. Technol. **22**, 85 (1999); A. M. Rosenfeld and R. S. Timsit, Q. Appl. Math. **39**, 405 (1981).
[13]Y. Y. Lau and W. Tang, J. Appl. Phys. **105**, 124902 (2009).
[14]M. R. Gomez, D. M. French, W. Tang, P. Zhang, Y. Y. Lau, and R. M. Gilgenbach, Appl. Phys. Lett. **95**, 072103 (2009).
[15]P. Zhang and Y. Y. Lau, J. Appl. Phys. **108**, 044914 (2010).
[16]D. A. Chalenski, B. R. Kusse, and J. B. Greenly, Phys. Plasmas **16**, 082707 (2009); M. R. Gomez, J. C. Zier, R. M. Gilgenbach, D. M. French, W. Tang, and Y. Y. Lau, Rev. Sci. Instrum. **79**, 093512 (2008).
[17]F. B. Hilderbrand, *Advanced Calculus for Applications* (Prentice-Hall, Englewood, 1962), p. 574.
[18]See http://www.ansoft.com for MAXWELL 3D software.